PAPER

Check for updates

Structural control and functionalization of thermoresponsive nanogels: turning cross-linking points into anchoring groups†

Alexis Wolfel, [iD] *[a] Huiyi Wang, [iD] [b] Ernesto Rafael Osorio-Blanco, [iD] [b] Julian Bergueiro, [iD] [c] Marcelo Ricardo Romero, [iD] [a] Cecilia Inés Alvarez Igarzabal [iD] [a] and Marcelo Calderón [iD] *[b,d]

Advancements in nanogel (NG) applications require precise control over their size, structure, and functionalization. However, synthesis methods have limitations that hinder the incorporation of some functional groups and hamper the architectural control over NGs. In this work, we developed a facile post-synthesis reaction strategy to modify the structure and functionalization of thermoresponsive NGs. Specifically, we studied the incorporation of a cleavable crosslinker, (+)-N,N′-diallyltartardiamide (DAT), in the synthesis of poly(N-isopropylacrylamide) (p-NIPAm), poly(N-isopropylmethacrylamide) (p-NIPMAm), and p-NIPAm-co-NIPMAm-based NGs. The efficient cleavage of DAT-crosslinks by sodium periodate enables control over the crosslinking degree and architecture of the NGs. This cleavage reaction also introduces alpha-oxoaldehydes (glyoxylic groups), which can be used for subsequent bio-conjugation under mild conditions. The incorporation of DAT-crosslinks in the NG architecture is governed by the reactivity of monomers and crosslinkers, as well as the initiation method used. Consequently, the structural changes caused by the cleavage of DAT-crosslinks depend on the composition and synthesis parameters, providing a valuable tool for fine-tuning drug delivery nanodevices in a post-synthetic step. As proof of concept, we demonstrated that the cleavage of DAT-crosslinks increased the loading efficiency of bovine serum albumin, a macromolecular drug surrogate. Additionally, we used the obtained alpha-oxoaldehydes to covalently link doxorubicin (DOXO) through hydrazone bonds, introducing pH-selective drug release.

Introduction

Nano-sized hydrogels (nanogels, NGs) require precise control over their architecture to succeed in different applications.[1,2] Structure, composition, size, and functional group distribution might need to be adapted to each specific biomedical purpose.[1,3–7] However, the synthetic methodologies often impose limitations to achieve the desired composition, spatial distribution of functional groups, mechanical and swelling properties, and structure.

Thermoresponsive NGs are often synthesized by a radical polymerization reaction known as precipitation polymerization.[2] This strategy however has some limitations when NGs with controlled architectures are needed. The incorporation of different monomers into the NGs is determined by parameters such as the relative reactivity between monomers and crosslinkers, the hydrophilicity of the formed oligomers, the concentration of the different species in the reaction media and the reaction initiation rates. These parameters not only directly affect nanoparticle size and polydispersity, but also component spatial distribution along the NG structure.[8–11] Thus, to achieve an application designed architecture, it is often necessary to apply post-polymerization modifications,[9,12] and/or strategies for structural control such as seeded precipitation polymerization, semi-batch synthesis, controlled radical polymerizations, among others.[1,2,13] Therefore, methods developed to control NGs architecture and functionalization are valuable tools to fine tune NGs properties. Besides achieving specific

[a]IPQA-CONICET, Laboratorio de Materiales Poliméricos, Departamento de Química Orgánica, Universidad Nacional de Córdoba, Córdoba, Argentina.
E-mail: awolfel@fcq.unc.edu.ar
[b]POLYMAT, Applied Chemistry Department, Faculty of Chemistry, University of the Basque Country, UPV/EHU, Paseo Manuel de Lardizabal 3, 20018 Donostia-San Sebastián, Spain. E-mail: marcelo.calderon@polymat.eu
[c]Centro Singular de Investigación en Química Bioloxica e Materiais Moleculares (CIQUS), Departamento de Química Orgánica, Universidade de Santiago de Compostela, 15782 Santiago de Compostela, Spain
[d]IKERBASQUE, Basque Foundation for Science, 48009 Bilbao, Spain
†Electronic supplementary information (ESI) available. See DOI: https://doi.org/10.1039/d3py00347g

structural characteristics for certain applications, such techniques also serve to explore key structure–property relationships.[7]

Recently, we used (+)-N,N′-diallyltartardiamide (DAT), a commercially available crosslinker, to achieve post-synthetic structural modification and functionalization of hydrogels.[14] This strategy was possible thanks to DAT's vicinal hydroxyl groups which can be efficiently cleaved by periodate, thus changing the crosslinking degree, and simultaneously generating valuable α-oxoaldehyde functional groups. Generally, the functionalization of synthetic polymers with aldehydes is limited by the instability of this functional group under polymerization conditions. To overcome this limitation, it is necessary to use aldehyde protecting groups (i.e., by forming acetals),[15] which increase the number of reaction steps. In contrast, the periodate-mediated cleavage of DAT-crosslinks in hydrogels yields α-oxoaldehydes by a simple and fast reaction in water. Moreover, α-oxoaldehydes have been described to undergo selective bio-orthogonal reactions under mild physiological conditions, which has been advantageous for the modification of proteins and peptides with high yields.[16,17] Therefore, the incorporation of DAT into NGs could be strategic for obtaining tailored NGs architectures and useful functional groups otherwise not accessible with the current synthetic methodologies.

In this work we studied the incorporation of DAT into thermosensitive NGs as a strategy to control their architecture and functionalization in a two-step process that consists of synthesis and post-synthetic modification. We observed that the incorporation of DAT along the NGs structure is significantly affected by the nature of the monomers (NIPAm and NIPMAm) but also depends on the initiation method applied during the synthesis. Moreover, the post-synthetic cleavage of DAT-crosslinks substantially changes NGs architecture and functionalization which may become a useful tool to control NGs' properties. As proof of concept, we show how the cleavage of DAT-crosslinks modifies the loading efficiency of a biomacromolecule. In addition, we exploited the utility of the obtained α-oxoaldehyde functional groups to covalently link doxorubicin (DOXO) through hydrazone bonds for pH-sensitive drug release. In essence, the incorporation of DAT into NGs is a useful tool to control NGs architectures and to promote valuable functionalization through an easy protocol.

Experimental

Reagents

The monomers N-isopropylacrylamide (NIPAm) (Sigma-Aldrich) and N-isopropylmethacrylamide (NIPMAm) (Sigma-Aldrich) were recrystallized from hexane to eliminate the stabilizing reagent before use. The agents N,N′-methylenebis(acrylamide) (BIS); (+)-N,N′-diallyltartardiamide (DAT) (Sigma-Aldrich); N,N,N′,N′-tetramethylethylenediamine (TEMED) (Sigma); ammonium persulfate (APS) (Anedra); sodium dodecyl sulphate (SDS) (Anedra); sodium periodate (Sigma-

Aldrich); adipic acid dihydrazide (AADH) (Anedra), doxorubicin hydrochloride (DOXO) (Sigma-Aldrich) were used as purchased. All the aqueous solutions were prepared with ultrapure water (18 MΩ cm^{-1}) from a Millipore Milli-Q® water purification system.

Nanogel synthesis

Thermosensitive NGs were synthesized as follows: the monomer (1×10^{-3} mol), the respective crosslinkers (DAT 0 to 15%mol and BIS 1.5%mol) and SDS (1.6×10^{-5} mol) where dissolved in 5 mL of ultrapure water (final monomer concentration = 0.2 M). The solution was deoxygenated by N$_2$ bubbling during 10 min. Then, in cases in which TEMED was used, 0.25 mL of deoxygenated TEMED (0.32 M) were added. This solution was heated up to 70 °C under magnetic stirring (350 rpm) for 5 min. Subsequently, 0.25 mL of deoxygenated APS solution (7.8×10^{-2} M) were added. The reaction was stirred at 70 °C during 4 h. The products were purified by dialysis (Spectra/Por® 6 Standard RC, 50 kDa molecular weight cut off [MWCO] dialysis bag), with reiterated water refreshing, at room temperature, during 48 h. The obtained NGs were named according to their composition as summarized in Table 1.

Nanogel modification using sodium periodate

The purified NGs, dispersed in water solutions, were treated with sodium periodate. A two-fold excess of sodium periodate with respect to the moles of DAT ($m_{NaIO_4} = 2 \times m_{DAT}$) was estimated considering eqn (1).

$$m_{DAT} = \frac{m_{DAT_i}}{V_f} \times V \qquad (1)$$

where m_{DAT_i} refers to moles of DAT used during the synthesis; V_f is the final volume of the solution during the synthesis and V is the volume of NG solution to be treated with periodate. After two hours of reaction at room temperature and under mechanical stirring, the NGs were purified by dialysis (Spectra/Por® 6 Standard RC, 50 kDa MWCO dialysis bag), with reiterated water refreshing, during 48 h.

Dynamic light scattering (DLS)

DLS experiments were performed in a Nano-ZS 90 Malvern equipped with a He–Ne (λ = 633 nm) laser measuring the light dispersed at an angle of 173°. The samples were prepared with freeze-dried NGs resuspended in distilled water with a concentration of 1 mg mL^{-1}. Each sample was maintained at 20 °C at least 20 min before the measurement, time observed to be enough to reach the thermal stability of the system.

Transmission electron microscopy (TEM)

Samples were prepared by depositing 5 µL of NG solution (0.1 mg mL^{-1}) over a carbon film coated copper grid (300 mesh, QUANTILOF). Later, 5 µL of uranyl acetate solution (1% w/v) were added and kept for 60 s. The excess of contrast reagent was removed, and the sample was dried at room temperature. For the measurement, a high-resolution transmission

Table 1 Feed composition of synthesized NGs and their respective hydrodynamic diameter (D_H) before and after treatment with periodate

| Sample | BIS (mol%) | DAT (mol%) | APS$_T$ | | | | APS$_{TEMED}$ | | | |
| | | | Untreated | | After NaIO$_4$ | | Untreated | | After NaIO$_4$ | |
			D_H (nm)	PDI	D_H (nm)	PDI	D_H (nm)	PDI	D_H (nm)	PDI
NB	1.5	0	138	0.12	138	0.11	182	0.10	177	0.09
NBD8	1.5	8	113	0.12	145	0.14	211	0.18	179	0.07
NBD10	1.5	10	84	0.05	132	0.13	203	0.23	168	0.08
NBD12	1.5	12	90	0.11	118	0.16	204	0.24	167	0.09
NBD15	1.5	15	109	0.11	134	0.14	275	0.40	126	0.13
NMB	1.5	0	159	0.07	158	0.09	PD	PD	PD	PD
NMBD8	1.5	8	253	0.01	242	0.08	139	0.29	PD	PD
NMBD10	1.5	10	139	0.02	143	0.11	150	0.23	PD	PD
NMBD12	1.5	12	127	0.05	134	0.12	157	0.21	PD	PD
NMBD15	1.5	15	134	0.05	149	0.12	172	0.09	PD	PD
NcoNMB	1.5	0	PD	PD	PD	PD	PD	PD	PD	PD
NcoNMBD8	1.5	8	281	0.02	371	0.01	414	0.06	PD	PD
NcoNMBD10	1.5	10	271	0.01	360	0.03	451	0.05	PD	PD
NcoNMBD12	1.5	12	258	0.01	347	0.03	403	0.04	PD	PD
NcoNMBD15	1.5	15	247	0.01	337	0.03	354	0.08	PD	PD

N = NIPAm; B = BIS; D = DAT; NM = NIPMAm. D_H was determined by DLS as the mean intensity value of three consecutive measurements at 20 °C. PD refers to samples that where too polydisperse to ensure an accurate D_H determination.

electron microscope TECNAI G2 20 TWIN was operated at 200 kV in transmission mode.

Cloud point temperature (T_{CP})

The cloud point temperature (T_{CP}) of the NGs was determined by measuring the change in optical transmittance ($\%T$) at different temperatures. A Cary 100 Bio UV-Visible equipment with a 6-slot chamber with controlled temperature was employed. The NGs aqueous solutions (1 mg mL^{-1}) were warmed up at 0.2 °C min^{-1} from 20 to 55 °C and the $\%T$ at 500 nm recorded (10 mm path length) while the internal temperature of the samples was measured by a thermocouple. The T_{CP} was considered as the global minimum of the first derivative of the function of $\%T$ with the temperature. Three cycles of heating–cooling were performed for each sample.

^{1}H-Nuclear magnetic resonance (^{1}H-NMR)

^{1}H-NMR spectrums were acquired in a JEOL ECX400 equipment. Approximately 10 mg of freeze-dried sample were resuspended in 0.5 mL of D$_2$O 24 h before each measurement. Samples were measured at 20 °C.

Loading of albumin

The encapsulation of bovine serum albumin labelled with fluorescein (BSA-FITC, Sigma Aldrich) was studied as a model biomacromolecular drug. For this purpose, dialyzed and freeze-dried NGs (1 mg) were re-dispersed in BSA-FITC solutions (phosphate buffered saline, pH 7.4) of different concentration, during 24 h at temperatures between 6–8 °C. Then, the solutions were purified by centrifugation (10 min at 6000 rpm; Sartorius, Göttingen, Germany) inside Vivaspin® devices (300 kDa MWCO). The amount of encapsulated BSA-FITC was determined by measuring the optical absorbance at 492 nm

together with a calibration curve made of BSA-FITC solutions. All the measurements were performed by quadruplicate.

Loading efficiency of the systems was calculated according to eqn (2):

$$LE\% = \frac{n_{BSA_T} - n_{BSA_f}}{n_{BSA_T}} \times 100 \qquad (2)$$

where n_{BSA_T} is the BSA-FITC number of moles used initially in the incubating solution and n_{BSA_f} is the free BSA-FITC which remained in the solution after the centrifugation (non-encapsulated).

Loading capacity of the systems was calculated according to eqn (3):

$$LC\% = \frac{m_{BSA_i}}{m_T} \times 100 \qquad (3)$$

where m_{BSA_i} is the mass of BSA-FITC incorporated into the nanodevice and m_T is the total mass of the nanodevice (NG + load).

Modification of nanogels with adipic acid dihydrazide (NBD-HDZ)

p-NIPAm NGs (NBD10) were treated with sodium periodate to yield α-oxoaldehydes. The product was then purified through dialysis using the aforementioned method. Following, NGs were modified with adipic acid dihydrazide (AADH). An excess of the hydrazide was used, with respect to the α-oxoaldehydes, to avoid the formation of crosslinks between NGs and promote the functionalization. The number of moles of added AADH was estimated as $m_{AADH} = 5 \times m_{DAT}$. The reaction was performed during 4 h at room temperature under mechanical stirring (350 rpm) in a sodium acetate buffer solution (pH = 5.3; concentration 0.02 M; ionic strength = 0.06 M). Later, the product was purified by dialysis (Spectra/Por® 6 Standard RC,

50 kDa MWCO dialysis bag) with repeated phosphate buffer changes (pH = 7.3; concentration 0.02 M; ionic strength = 0.06 M) during 72 h.

Conjugation and release of doxorubicin (DOXO)

For DOXO immobilization, NBD-HDZ and NBD (control) NGs were diluted (3 mg mL^{-1}) into 4.5 mL PBS solution (pH = 6.5; 10 mM). Then, 0.5 ml dimethylformamide (DMF) solution containing 3 mg of DOXO hydrochloride was added. The reaction was performed overnight, under mildly stirring, at room temperature and protected from light. Afterwards, the mixture was purified by dialysis (Spectra/Por® 6 Standard RC, 50 kDa MWCO dialysis bag) in phosphate buffer (pH = 7.4, 10 mM).

To study DOXO release at different pH values, 0.5 mL of NGs-DOXO solution was added into phosphate buffer pH 2.8 or 7.4. The solution was mildly stirring for 1 h at room temperature and protected from light. After the incubation, the mixture was dialyzed (Spectra/Por® 6 Standard RC, 50 kDa MWCO dialysis bag) for 3 days in phosphate buffer with the corresponding pH value of 2.8 and 7.4 and measured by UV-Vis absorption to quantify the amount of unreleased DOXO. The amount of DOXO in NGs, before and after release experiments, was calculated by measuring NGs-DOXO absorbance at λ = 495 nm and contrasted with a calibration curve made by DOXO solutions.

The cumulative release of DOXO was calculated according to eqn (4):

$$\text{DOXO release} \% = \frac{m_{\text{DOXO}_E} - m_{\text{DOXO}_U}}{m_{\text{DOXO}_E}} \times 100 \qquad (4)$$

where m_{DOXO_E} is the mass of encapsulated DOXO in the NGs and m_{DOXO_U} is the unreleased DOXO after incubation at different pH values.

UV-Visible

Measurements were performed using a Shimadzu UV-1800 equipment. The absorbance spectra (all in buffer solution pH = 7.4) were measured at 20 °C between 700–300 nm.

Results and discussion

Incorporation of DAT into thermoresponsive NGs

We propose to incorporate DAT, a crosslinker that can be cleaved by periodate, as a tool to produce nano-structural changes and aldehyde functional groups in p-NIPAm and p-NIPMAm based NGs. For this reason, we studied how DAT incorporation along the NGs structure depends on the monomer/crosslinkers reactivity and the polymerization initiation conditions (Fig. 1).

p-NIPAm, p-NIPMAm and p-NIPAm-*co*-NIPMAm based NGs were synthesized *via* precipitation polymerization, using a fixed amount of BIS (1.5 mol%) and variable compositions of DAT (0–15 mol%) (Table 1). BIS was included in all formulations to introduce non-cleavable crosslinking points to prevent complete degradation of the NGs after cleavage of DAT-crosslinks. To evaluate the effect of different initiation conditions in DAT incorporation, two initiation strategies were applied: the thermal decomposition of APS (APS$_T$) and the redox promoted decomposition of APS in the presence of TEMED (APS$_{\text{TEMED}}$).

The D_H of the NGs, determined by DLS as the mean intensity value at 20 °C, was dependent on the nature of monomers (NIPAm, NIPMAm, or NIPAm-*co*-NIPMAm) and the initiation conditions. For instance, NIPAm-based NGs initiated by APS$_T$ ranged from 84 to 109 nm while NIPAm-based NGs initiated by APS$_{\text{TEMED}}$ showed values between 182 to 275 nm. For NIPMAm-based NGs, the ranges were 127–253 nm and 139–198 nm when synthesized by APS$_T$ or APS$_{\text{TEMED}}$, respectively. For copolymeric mixtures of NIPAm and NIPMAm, sizes
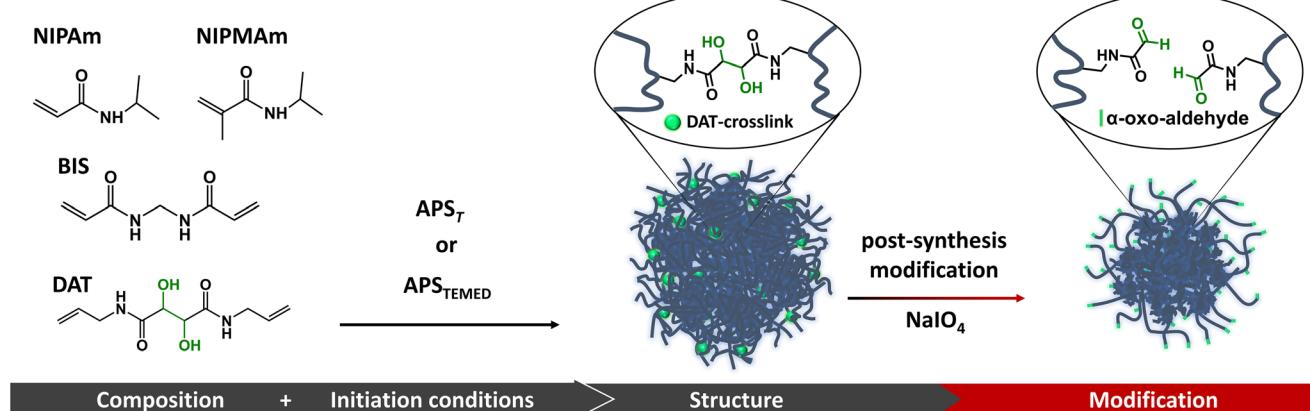
Fig. 1 Study design. The reactivity of monomers and crosslinkers, along with the conditions of the polymerization initiation, determine the final distribution of DAT and BIS within the structure of the NGs. This spatial distribution then influences the changes in NGs properties that occur after post-synthetic cleavage of DAT-crosslinks.

ranged from 247 to 281 nm when synthesized by APS_T and from 354 to 451 nm when APS_{TEMED} was used. In general, larger D_H are obtained when APS_{TEMED} is used instead of APS_T. The difference in size ranges indicate that the structure of NGs may vary under different initiation conditions and according to monomer nature. Furthermore, the observed size differences may be directly (but not only) related to a differential incorporation of the crosslinkers BIS and DAT in the different formulations, leading to different crosslinking degrees and NG's architectures.

Furthermore, we studied the changes in NGs properties caused by the cleavage of DAT-crosslinks. DAT-crosslinks were cleaved through a fast and efficient reaction in aqueous $NaIO_4$ solution and changes in NGs properties were studied by DLS and TEM.[18]

After the cleavage of DAT-crosslinks we observed changes in D_H and morphology that correlates to the initial incorporation of DAT along the NG structure under different reaction conditions (Fig. 2). For instance, NGs synthesized in APS_T showed smaller D_H shift than those synthesized in APS_{TEMED}. The D_H of APS_T-initiated NGs increased after periodate treatment (e.g., 22 to 58% for NIPAm NGs), whilst in APS_{TEMED}-initiated NGs either decreased (up to 217% in p-NIPAm NGs) or particles were completely degraded (p-NIPMAm NGs). Thus, it is

evident that the initiation method (APS_T vs. APS_{TEMED}) influenced the incorporation of the crosslinkers. Furthermore, DAT seems to play a more structural and cohesive role after APS_{TEMED} initiation than after APS_T polymerizations, presumably by aggregating small particles during particle growing. Comparable results have been reported for BIS-crosslinked p-NIPAm NGs that indicated an early participation of the crosslinker on particle nucleation,[19] specially at higher concentrations of the crosslinker, when synthesized via APS_{TEMED}.[20,21] Compared to APS_T, TEMED promotes a faster generation of radicals during synthesis[22] and has a role as chain transfer reagent.[20,21] These aspects may have effects in the number of growing particles, their charge density, and their colloidal stability, ultimately defining the incorporation of the components in the NGs, and their final size and architecture.[20,21] In addition, it may be considered that DAT is an allyl crosslinker. Generally, allyl groups are likely to undergo monomer chain transfer reactions, which often leads to the obtainment of middle-molecular weight polymer chains (in contrast to the large molecular weights commonly obtained with vinyl monomers) and can lead to low conversion efficiency.[23] Furthermore, an increment in the concentration of initiator can lead to a shortening of chain length (low degree of polymerization) but increases the conversion efficiency in allyl
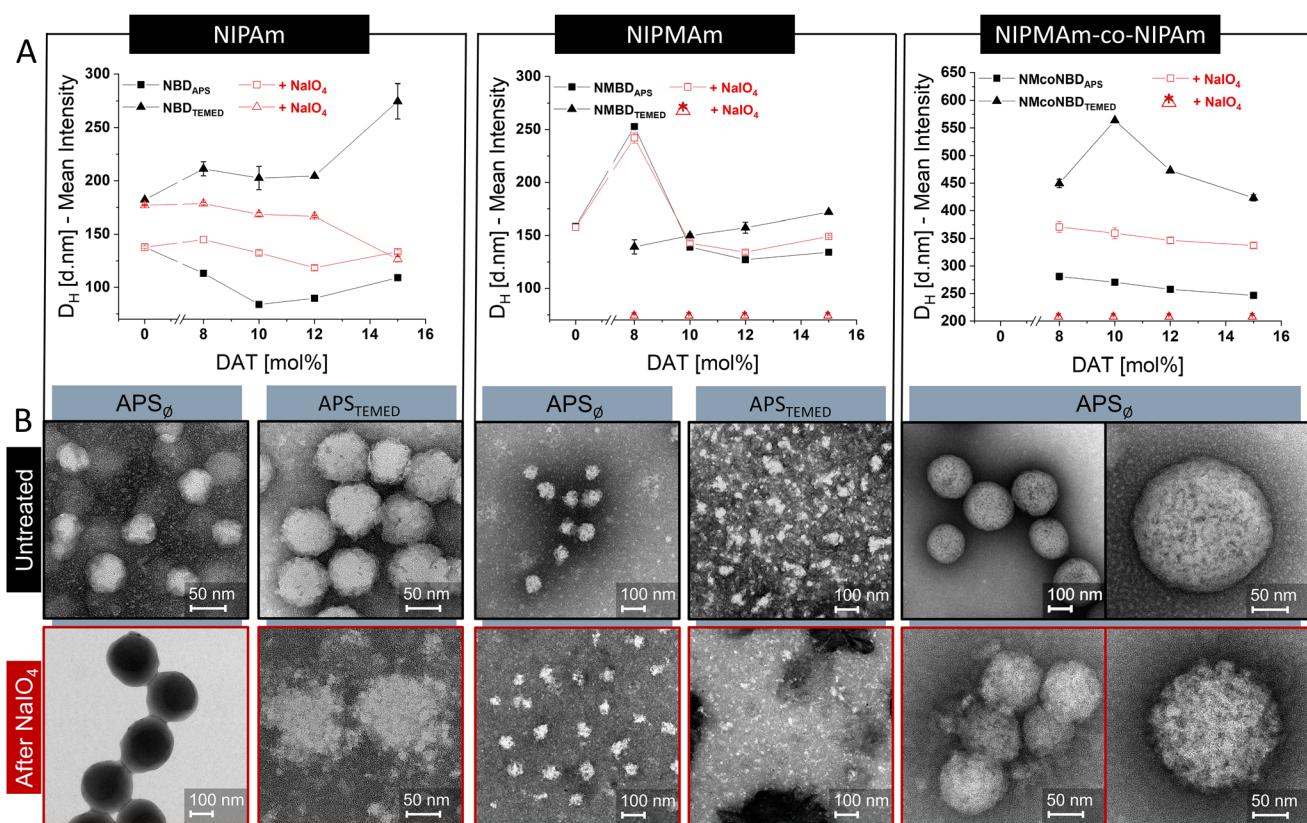

Fig. 2 (A) Hydrodynamic diameter (D_H) of NGs obtained by the thermal decomposition of APS (black, squares) and the redox couple APS/TEMED (black, triangles). D_H of the NGs after post-synthesis modification with sodium periodate is shown by red empty symbols. D_H was determined by DLS as the mean intensity value at 20 °C. Error bars denote the mean standard deviation for 3 consecutive DLS measurements. (B) TEM images of NGs before (upper row) and after (down row) $NaIO_4$ treatment.

polymerization.[24] Therefore, it is possible that the faster generation of radicals produced by TEMED, in comparison to APS_T, could modify the efficiency of DAT incorporation, as well as polymer architecture. Our results suggested that APS_{TEMED} initiation promoted a more structurally relevant role of DAT as a crosslinker in the nanogels than APS_T. It could be speculated that the faster production of radicals with APS_{TEMED} initiation leads to an increase in the efficiency of incorporation of DAT at the initial stages of polymerization, thus causing a more structural role of the crosslinker in particle nucleation.

Morphological analysis by TEM supported the previous observations. Although noticeable structural changes were promoted in APS_T initiated NGs after treatment with periodate (Fig. 2B; S1, 2†), they were relatively small in comparison to NGs synthesized via APS_{TEMED} (Fig. 2B; S3†). The last showed either a globular to fuzzy structure change or a complete degradation, depending on NG composition.

NGs synthesized with different monomers (either NIPAm or NIPMAm) showed a completely different morphological change after cleavage of DAT-crosslinks. This suggests that BIS and DAT are differently incorporated when a different monomer is used. On the one hand, p-NIPAm-based NGs always maintained a globular structure after treatment with periodate (Fig. 2; S1, S3†). This implies that, after cleavage of DAT-crosslinks, BIS-crosslinks keep the globular structures together. This observation is in line with the reported incorporation of BIS in p-NIPAm NGs which takes place during early phase of particle maturation creating highly crosslinked cores.[19,25] On the other hand, p-NIPMAm-based NGs either underwent a large change in D_H or lost completely their globular structure upon cleavage of DAT-crosslinks, indicating little participation of BIS in NGs globular architecture (Fig. 2; Table 1; Fig. S2†). It has been reported that the differential reactivity between BIS and NIPMAm is responsible for little incorporation of the crosslinker into p-NIPMAm NGs.[26,27] However, we noticed that this is mostly the case only when the reaction was initiated by APS_{TEMED}. When p-NIPMAm NGs were initiated via APS_T, they maintained a globular structure after DAT-crosslinks cleavage.

In summary, the difference in reactivity of monomers and crosslinkers plays a very important role in the final distribution of crosslinks along the NGs architecture. Furthermore, this distribution can be greatly affected by the free radical initiation method, which will alter the kinetics of particle growth, nucleation and maturing.

To further understand our results, it is important to consider that p-NIPAm NGs have been reported to undergo self-crosslinking at the periphery creating a crosslinked-shell.[25,28-30] Self-crosslinking only occurs in p-NIPAm NGs under APS_T initiation and is minimized by the presence of TEMED.[30] On the contrary, the methyl groups in p-NIPMAm prevent the formation of those self-crosslinks in p-NIPMAm NGs.[25] Self-crosslinking may contribute to the moderate morphological change observed in NIPAm-based NGs synthesized in APS_T as compared to other NGs (Fig. 2).

Regarding DAT incorporation, it has been reported that its reactivity is lower than that of BIS for acrylamide co-polymeriz-ation.[31] In addition, DAT may form hydrophilic[32] and soluble polymer chains. Therefore, it is expected that DAT-containing hydrophilic chains will be incorporated towards the outer shells of NGs architecture when compared to BIS incorporation which is expected to be at the core (at the initial stages of particle maturing during a precipitation polymerization).[19,25,33] This differential incorporation of BIS and DAT was more evident when synthesizing p-NIPAm NGs compared to p-NIPMAm NGs, probably due to the previously mentioned difference in BIS incorporation due to NIPAm and NIPMAm reactivity. It is noteworthy that the scenario changes when APS_{TEMED} is used as initiator, promoting an earlier participation of DAT and a more structural role in particle nucleation.

p-NIPAm-co-NIPMAm copolymers showed remarkable architectural changes after DAT-cleavage. NGs synthesized via APS_T increased HD approx. 32% with globular shape greatly preserved (Fig. 2). Moreover, nanosized openings were observed within the globular particles, resembling a porous architecture. It has been reported that p-NIPAm-co-NIPMAm NGs display a nanophase separated internal morphology which consists of nanosized p-NIPAm domains within p-NIPMAm regions in a "dirty snowball" array.[34] Our NGs were synthesized in equivalent conditions to those reported and it is likely that they may exhibit a similar architecture. Still, the incorporation of the cleavable crosslinker may alter the NG structure. If nanophase separation is taking place, BIS and DAT may also be incorporated to a different extent within the NG different phases, just as they were differently incorporated in the homo-polymeric NGs. Although this hypothesis has yet to be confirmed, nanophase separation may be responsible for the generation of the observed nanosized openings. Conceptually, having localized cleavable crosslinks in nanophase separated microgels may be of interest to further modify and control their architecture for drug delivery applications.

The previous results indicate that DAT crosslinks can be utilized for post-synthetic modification of NGs architecture. The incorporation of DAT was found to be influenced by reaction conditions and monomer reactivity, which can be manipulated to induce various DAT-crosslinked NGs structures and subsequent post-synthetically modified architectures. Since DAT-cleavage likely alters the crosslinking degree of NGs and introduces valuable functional groups, it could be used as a versatile tool to optimize the properties of NGs for drug delivery applications, as evidenced in the following sections.

Effect of the structural change on the loading of a macromolecular cargo

The structure of a nanoparticle plays an important role on the loading and release of bioactives for drug delivery applications. It could affect, for example, the diffusion of the cargoes through the network pores of the nanodevice.[35-37] Since only a few scarcely available techniques can give valuable structural information about NGs (e.g., small-angle neutron scattering), these aspects have not been deeply explored. We envisioned that our strategy to promote changes in architecture and cross-linking degree of NGs may have an impact in drug loading and

become a tool to improve the loading of macromolecules into the NGs. As a proof of concept, we studied the loading of bovine serum albumin (BSA) as a macromolecular model drug. We loaded a fluorescently labelled albumin (BSA-FITC) into p-NIPAm-co-NIPMAm NGs before and after DAT-crosslinks cleavage. These NGs previously showed an increase in D_H after DAT-crosslinks cleavage while maintaining a low PDI and spherical morphology (Table 1; Fig. 2). We compared the loading of BSA-FITC in NGs synthesized with 8 and 15 mol% DAT (NMcoNBD8 and NMcoNBD15, respectively) before and after their structural modification with periodate.

At high protein concentrations (e.g., 2 mg mL^{-1}) in the incubation media, we observed similar high loading efficiency (LE) and loading capacity (LC) in all compositions, with little difference between periodate treated and untreated samples (Fig. 3). However, under lower protein concentrations (e.g., 0.1 mg mL^{-1}) NGs showed a 20% increase in LE after DAT-crosslinks cleavage. An increase in LE following the cleavage of DAT-crosslinks could be attributed to an increase in their porosity. This could allow for greater protein penetration, as previously reported in literature.[37] This effect could have been further enhanced due to the generation of polar α-oxoaldehyde groups (Fig. S4 and 5†) and to possible changes in the surface charge of the particles, which could also have an effect in the interaction with the protein. Both NG compositions, with 8 and 15 mol% DAT, showed a similar increase in LE after modification with periodate, indicating that their pore size is not significantly different or that their differences do not impact selectivity for this particular protein. The obtained results demonstrate that the post-synthesis cleavage of DAT-crosslinks can significantly affect the loading of a macromolecular model drug into the NGs and therefore could be used as a tool for tunning the properties of nanoplatforms for drug delivery and to study structure–property relationships.

Doxorubicin covalent binding to NG backbone and further pH-triggered release

The periodate mediated cleavage of DAT-crosslinks leads to the formation of α-oxoaldehydes (glyoxylic groups) which could be further exploited for chemical derivatization and drug conjugation in hydrogels.[38] As a proof of concept, we used the α-oxoaldehydes to covalently attach the anti-cancer drug doxorubicin (DOXO) through hydrazone bonding (Fig. 4A). DOXO has been previously attached to drug delivery systems through hydrazone bonds to generate smart delivery devices.[39] Since hydrazone bonds can be cleaved under acidic conditions, the drug can be selectively released into acidic environments such as tumour microenvironment and intracellular lysosomal compartments. This approach has demonstrated to be a promising solution to avoid multidrug resistance during chemotherapy since the pH-selective release of DOXO avoids elimination mechanisms of the cells and the drug reaches the action site more efficiently than free DOXO.[40–42]

After treatment with periodate, the ^{1}H-NMR of p-NIPAm NGs showed a new signal at 5.26 ppm, indicating the presence of hydrated α-oxoaldehydes in the polymers (Fig. 4C).[38,43] Furthermore, the presence of polar α-oxoaldehyde groups promoted an increase in the cloud point temperature (T_{CP}) of the NGs (Fig. 4B).[44] Aldehyde-bearing NGs were then reacted with adipic acid dihydrazide (AADH) to create anchoring points for DOXO. We used diluted conditions and a large excess of AADH to ensure the modification of the aldehydes with one hydrazide end of the bifunctional AADH and avoid crosslinking between NGs (Fig. 4A). DLS showed no significant changes in the size distribution after modification with AADH which indicates no considerable interparticle crosslinking (Fig. S6†). Furthermore, the ^{1}H-NMR (Fig. 4C) spectrum showed the dis-
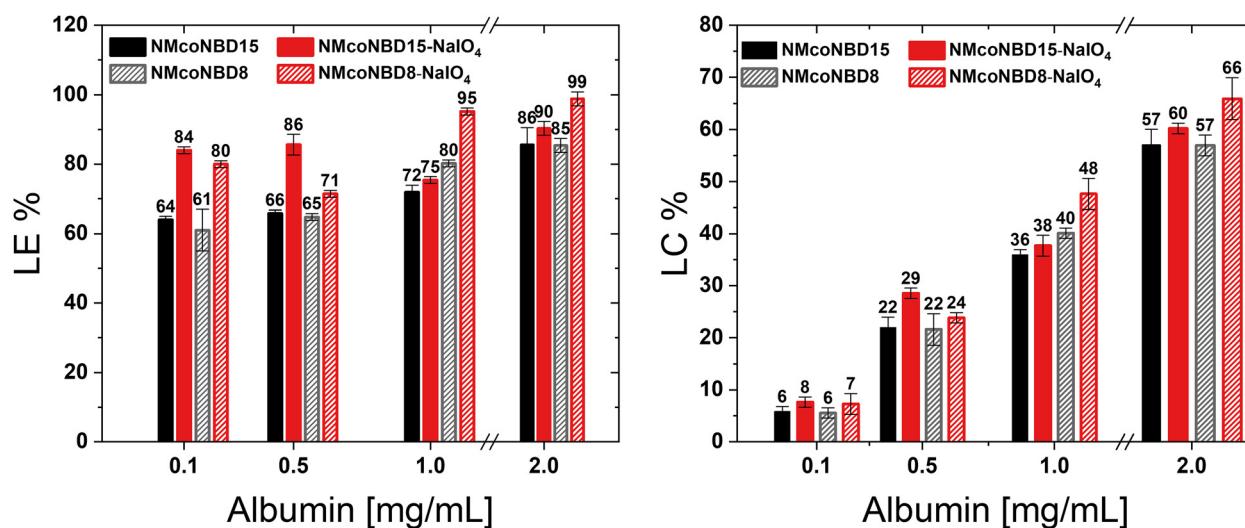
Fig. 3 Loading efficiency (LE%) and Loading capacity (LC%) of BSA-FITC into pristine p-NIPAm-co-NIPMAm-BIS-DAT NGs (black/grey) and NGs modified with periodate (red).
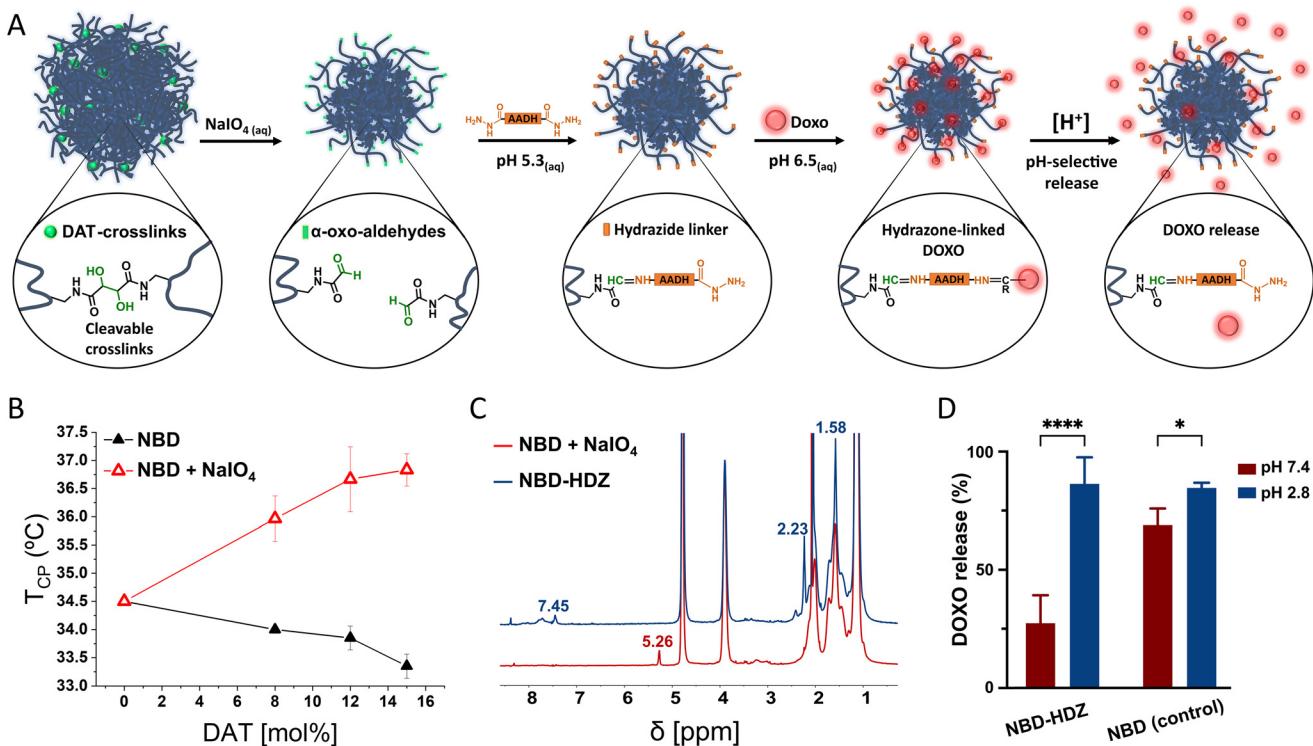
Fig. 4 DAT-crosslinks cleavage promotes the formation of α-oxoaldehydes which can be used for further chemical derivatization and drug loading. (A) Reactions performed at mild conditions for the immobilization of DOXO in thermoresponsive NGs. (B) T_{CP} values of p-NIPAm NGs before and after treatment with periodate. (C) ^{1}H-NMR of p-NIPAm NGs bearing α-oxoaldehydes functional groups (red) and after their modification with adipic acid dihydrazide (NBD-HDZ, blue). (D) DOXO cumulative release at different pHs for DOXO-loaded p-NIPAm NGs.

appearance of the α-oxoaldehyde characteristic signal (5.28 ppm) and appearance of new signals attributed to the protons of the hydro-carbonated chain of AADH (2.23 and 1.58 ppm); and the hydrazone bonds between AADH and α-oxoaldehydes (7.45 ppm).[38] Following, hydrazide-functionalized NGs and unmodified NGs (controls) were incubated with DOXO in a mild acidic PBS buffer (pH 6.5, 10 mM) during 12 h. NG-DOXO conjugates were purified by dialysis (PBS pH 7.4, 10 mM) for 3 days and characterized by UV-VIS (Fig. S8†).

The loading capacity was approximately three times higher in control groups than in hydrazone functionalized NGs (Fig. S8†), indicating that larger amounts of DOXO can be (physically) entrapped in control groups. This result could be a consequence of the structural change after the periodate treatment. However, control NGs showed a large unspecific release of DOXO at pH 7.4 (Fig. 4D). In contrast, hydrazone functionalized NGs improved the pH-selective release profile, minimizing the release of DOXO at neutral pH and boosting the release at acidic pH.

Altogether, these results proved that the incorporation of DAT as a cleavable crosslinker can be used as a strategy to modify the architecture of micro and nanogels and to promote the formation of α-oxoaldehydes without the requirement of protection and deprotection reaction steps. Furthermore, both the structural and chemical modification can be applied to tune the drug loading and release profiles of nanoplatforms.

Conclusions

The cleavable crosslinker (+)-N,N'-dialyltartardiamide (DAT) was incorporated in the synthesis of p-NIPAm, p-NIPMAm and p-NIPAm-co-NIPMAm NGs. The periodate-mediated cleavage of DAT-crosslinks triggered changes in architecture, hydrodynamic diameter, and functionalization of the NGs. It was found that the initiation method, either by APS thermal decomposition or by redox initiation with the accelerator TEMED, played a crucial role at determining the incorporation and localization of DAT-crosslinks along the NGs' architecture. In addition, the different reactivity of NIPAm and NIPMAm influenced the incorporation of the crosslinker.

The post-synthesis modification of DAT-crosslinked NGs was performed by a quick reaction in water and promoted changes in NGs' structure as well as yielding valuable α-oxoaldehydes. The structural modification showed a direct impact on the loading of albumin as a model protein, increasing the loading efficiency after the cleavage of DAT-crosslinks. Moreover, the obtained α-oxoaldehydes were advantageous for further chemical derivatization of the NGs through hydrazone bonds formed under mild conditions. This feature was exploited to conjugate DOXO and selectively release it under acidic conditions.

The herein presented strategy could become a useful tool to precisely tune NG's properties such as crosslinking density,

architecture, and functionalization. Moreover, α-oxoaldehydes groups are incorporated by a simple post-synthesis modification, which can facilitate (bio)conjugation under mild conditions.

Author contributions

This manuscript was written through contributions of all authors. All authors have given approval to the final version of the manuscript.

Conflicts of interest

There are no conflicts to declare.

Acknowledgements

References

1 I. Neamtu, A. G. Rusu, A. Diaconu, L. E. Nita and A. P. Chiriac, *Drug Delivery*, 2017, **24**, 539–557.

2 M. Karg, A. Pich, T. Hellweg, T. Hoare, L. A. Lyon, J. J. Crassous, D. Suzuki, R. A. Gumerov, S. Schneider, I. I. Potemkin and W. Richtering, *Langmuir*, 2019, **35**, 6231–6255.

3 M. Asadian-Birjand, A. Sousa-Herves, D. Steinhilber, J. C. Cuggino and M. Calderon, *Curr. Med. Chem.*, 2012, **19**, 5029–5043.

4 T. Hoare and R. Pelton, *Langmuir*, 2008, **24**, 1005–1012.

5 J. C. Cuggino, E. R. O. Blanco, L. M. Gugliotta, C. I. Alvarez Igarzabal and M. Calderón, *J. Controlled Release*, 2019, **307**, 221–246.

6 Z. Li, C. Xiao, T. Yong, Z. Li, L. Gan and X. Yang, *Chem. Soc. Rev.*, 2020, **49**, 2273–2290.

7 V. K. Switacz, S. K. Wypysek, R. Degen, J. J. Crassous, M. Spehr and W. Richtering, *Biomacromolecules*, 2020, **21**, 4532–4544.

8 J. Wei, Y. Li and T. Ngai, *Colloids Surf., A*, 2016, **489**, 122–127.

9 A. Pich and W. Richtering, *Polymer Nanogels and Microgels*, Elsevier B.V., 2012, vol. 6.

10 L. C. Kröger, W. A. Kopp and K. Leonhard, *J. Phys. Chem. B*, 2017, **121**, 2887–2895.

11 T. Hoare and D. McLean, *J. Phys. Chem. B*, 2006, **110**, 20327–20336.

12 M. N. Leiske, R. Singha, S. Jana, B. G. De Geest and R. Hoogenboom, *Polym. Chem.*, 2023, **14**, 2034–2044.

13 E. R. Osorio-Blanco, J. Bergueiro, B. E. Abali, S. Ehrmann, C. Böttcher, A. J. Müller, J. L. Cuéllar-Camacho and M. Calderón, *Chem. Mater.*, 2020, **32**, 518–528.

14 A. Wolfel, C. I. Alvarez Igarzabal and M. R. Romero, *Eur. Polym. J.*, 2020, **140**, 110038.

15 C. Negrell, C. Voirin, B. Boutevin, V. Ladmiral and S. Caillol, *Eur. Polym. J.*, 2018, **109**, 544–563.

16 O. El-Mahdi and O. Melnyk, *Bioconjugate Chem.*, 2013, **24**, 735–765.

17 R. J. Spears and M. A. Fascione, *Org. Biomol. Chem.*, 2016, **14**, 7622–7638.

18 A. Wolfel, M. R. Romero and C. I. Alvarez Igarzabal, *Polymer*, 2017, **116**, 251–260.

19 Y. Nishizawa, H. Minato, T. Inui, T. Uchihashi and D. Suzuki, *Langmuir*, 2021, **37**, 151–159.

20 O. L. J. Virtanen, H. M. Ala-Mutka and W. Richtering, *Macromol. Chem. Phys.*, 2015, **216**, 1431–1440.

21 O. L. J. Virtanen, M. Brugnoni, M. Kather, A. Pich and W. Richtering, *Polym. Chem.*, 2016, **7**, 5123–5131.

22 X. De Feng, X. Q. Guo and K. Y. Qui, *Makromol. Chem.*, 1988, **189**, 77–83.

23 S. Inoue, T. Kumagai, H. Tamezawa, H. Aota, A. Matsumoto, K. Yokoyama, Y. Matoba and M. Shibano, *J. Polym. Sci., Part A: Polym. Chem.*, 2011, **49**, 156–163.

24 A. Matsumoto, T. Kumagai, H. Aota, H. Kawasaki and R. Arakawa, *Polym. J.*, 2009, **41**, 26–33.

25 M. H. Smith, E. S. Herman and L. A. Lyon, *J. Phys. Chem. B*, 2011, **115**, 3761–3764.

26 B. Wedel, Y. Hertle, O. Wrede, J. Bookhold and T. Hellweg, *Polymers*, 2016, **8**, 162.

27 D. Duracher, A. Elaïssari and C. Pichot, *J. Polym. Sci., Part A: Polym. Chem.*, 1999, **37**, 1823–1837.

28 J. Gao and B. J. Frisken, *Langmuir*, 2003, **19**, 5212–5216.

29 X. Hu, Z. Tong and L. A. Lyon, *Langmuir*, 2011, **27**, 4142–4148.

30 O. L. J. Virtanen, A. Mourran, P. T. Pinard and W. Richtering, *Soft Matter*, 2016, **12**, 3919–3928.

31 C. Gelfi and P. G. Righetti, *Electrophoresis*, 1981, **2**, 213–219.

32 C. Gelfi, A. Alloni, P. de Besi and P. G. Righetti, *J. Chromatogr. A*, 1992, **608**, 343–348.

33 A. Vdovchenko, A. K. Pearce, M. Freeley, R. K. O'Reilly and M. Resmini, *Polym. Chem.*, 2021, **12**, 6854–6864.

34 M. Keerl, J. S. Pedersen and W. Richtering, *J. Am. Chem. Soc.*, 2009, **131**, 3093–3097.

35 L. Navarro, L. E. Theune and M. Calderón, *Eur. Polym. J.*, 2020, **124**, 109478.

36 L. E. Theune, R. Charbaji, M. Kar, S. Wedepohl, S. Hedtrich and M. Calderón, *Mater. Sci. Eng., C*, 2019, **100**, 141–151.

37 S. Nayak and L. A. Lyon, *Angew. Chem., Int. Ed.*, 2004, **43**, 6706–6709.

38 A. Wolfel, M. R. Romero and C. I. Alvarez Igarzabal, *Eur. Polym. J.*, 2019, **112**, 389–399.

39 S. J. Sonawane, R. S. Kalhapure and T. Govender, *Eur. J. Pharm. Sci.*, 2017, **99**, 45–65.

40 W. L. Ye, Y. P. Zhao, R. Na, F. Li, Q. B. Mei, M. G. Zhao and S. Y. Zhou, *J. Pharm. Sci.*, 2015, **104**, 2293–2303.

41 L. Qiu, J. Xu, K. S. Ahmed, M. Zhu, Y. Zhang, M. Long, W. Chen, W. Fang, H. Zhang and J. Chen, *Acta Biomater.*, 2022, **140**, 686–699.

42 B. Balcı and A. Top, *J. Polym. Res.*, 2018, **25**, 104.

43 E. B. Whipple, *J. Am. Chem. Soc.*, 1970, **92**, 7183–7186.

44 S. Lanzalaco and E. Armelin, *Gels*, 2017, **3**, 36.